

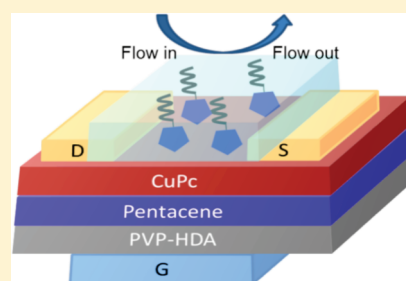
Pentacene Based Organic Thin Film Transistors as the Transducer for Biochemical Sensing in Aqueous Media

Hadayat Ullah Khan,^{*,†} Mark E. Roberts,[‡] Wolfgang Knoll,^{†,§} and Zhenan Bao^{*,‡}[†]Material Science Group, Max-Planck Institute for Polymer Research, Ackermannweg-10, D-55128 Mainz, Germany[‡]Department of Chemical Engineering, Stanford University, 381 North South Mall, Stanford, California 94305, United States[§]AIT Austrian Institute of Technology GmbH, Donau-City-Strasse 1, 1220 Vienna, Austria

S Supporting Information

ABSTRACT: Organic thin-film transistors show tremendous potential for versatile electronic sensors. Critical challenges facing the integration of organic thin-film transistors (OTFTs) as chemical and biological sensors include reproducibility, sensitivity, and particularly stability. Here, we describe a bilayer organic semiconductor structure consisting of a pentacene active layer with copper phthalocyanine as the top surface passivation layer. In this architecture, the copper phthalocyanine (CuPc) acts as a surface passivation layer with efficient charge injection into the pentacene layer, thus providing a versatile method for the incorporation of many semiconductor materials as the sensing element. OTFTs fabricated with the described structure exhibited a field-effect mobility of $1.15 \pm 0.2 \text{ cm}^2 \text{ V}^{-1} \text{ s}^{-1}$ at -2 V in ambient conditions with stable performance in aqueous media ($0.5 \text{ cm}^2 \text{ V}^{-1} \text{ s}^{-1}$ at -1 V). X-ray diffraction (XRD) confirms that the bilayer film achieves a high degree of molecular order as suggested by the high OTFT mobility. OTFTs based on the pentacene/CuPc bilayer films were fabricated on both rigid silicon and flexible polyimide substrates. The aqueous buffer stability of these devices was exploited for the detection of chemical and biological species.

KEYWORDS: organic electronics, low-voltage OTFTs, flexible OTFTs, transistor biosensors in aqueous medium



■ INTRODUCTION

Organic materials have shown tremendous promise for a variety of electronic components and devices, including organic light-emitting diodes (OLEDs),¹ organic photovoltaics,² radio frequency identification cards (RFIDs),³ and biosensors.^{4–6} The rapid progress of the field benefits from improvements in fabrication processes and new material design, with notable advances in improving the electronic properties of semiconducting⁷ and insulating^{8,9} materials. Organic thin-film transistors (OTFTs) have gained considerable attention due to their low cost, ease of manufacturing, compatibility with flexible, large area substrates, and numerous demonstrations of scalable patterning processes.^{6,10–15}

With many recent advances in chemical and biological detection, sensors based on organic semiconductors and OTFTs in particular are poised to provide a viable, low cost alternative to current mass spectrometry or optical detection systems.⁵ Avoiding optical excitation sources and detectors vastly reduces cost and allows for portability, and eliminating labeling steps simplifies the readout and increases the speed and ease of bioaffinity assays. There have been few examples demonstrated based on transistor sensor platform using stable organic semiconductors, in which the current passing through the semiconductor is mediated by either target analytes or ions from the electrolyte adsorbed to the film surface via nonspecific⁵ or specific interactions.⁴ One particular advantage of the use of a transistor as the readout device, as opposed to a simpler two terminal chemresistor, is the ability to modulate the drain current with a

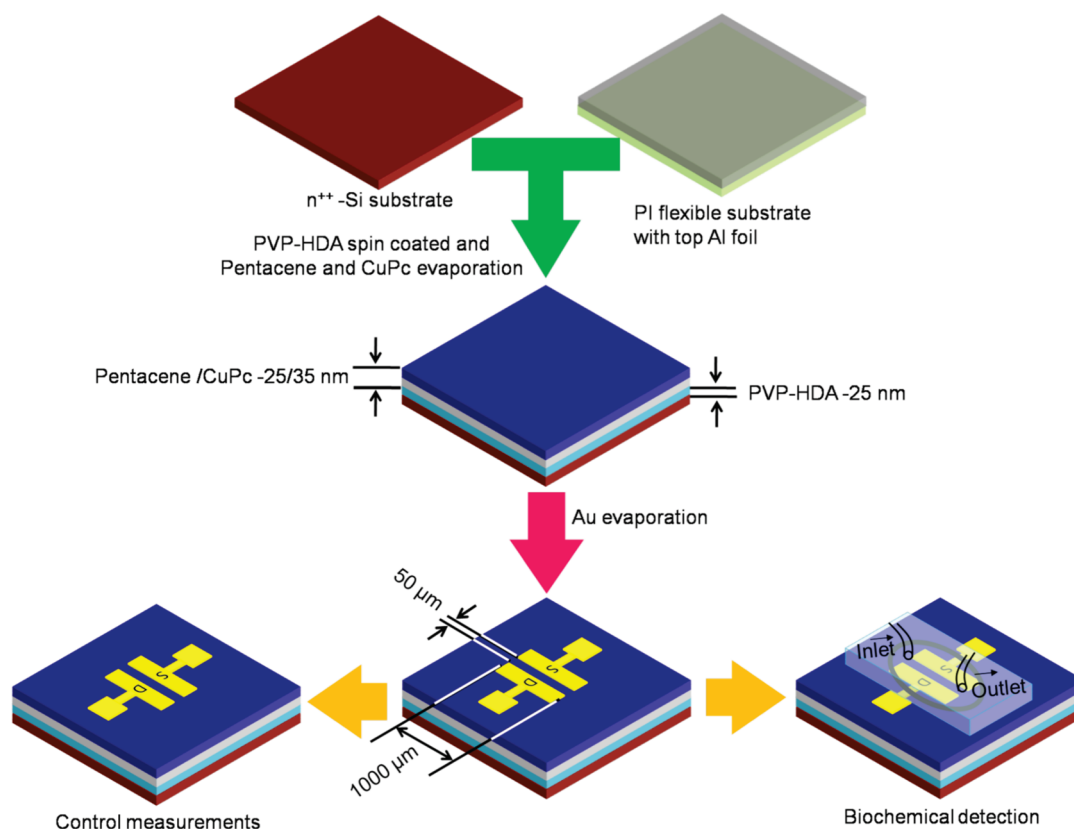
gate bias.¹⁶ Moreover, the utilization of organic materials offers the possibility of tuning the sensitivity¹⁷ and selectivity⁴ toward various analytes by chemical modification of the polymer backbone or the addition of side groups. Low-cost fabrication methods combined with large-area processing capabilities potentially allow for a means to produce large quantities and arrays of detection elements to measure multiple samples simultaneously. This technology represents an important step toward the realization of a high throughput and disposable detection methodology.

A few examples of electronic detection have been demonstrated using inorganic based silicon nanowires. Despite their high sensitivity and stability in aqueous media,^{18,19} their fabrication remains challenging, owing to the requirements of sophisticated lithography techniques to precisely place them. Solution processed inorganic thin-film devices may be promising; however, organic semiconductors benefit from relatively low temperature, solution processing capability, and the flexibility to work on any kind of substrate with a high mobility.^{20–22} The lifetime of unpassivated OTFTs is typically short under ambient conditions as many organic semiconductors degrade through reaction with oxygen, moisture, and/or light.²³ Although pentacene has attracted enormous interest as the active layer in OTFTs as a result of its high carrier transport properties,^{24,25} it suffers

Received: December 29, 2010

Revised: February 12, 2011

Published: March 02, 2011

Scheme 1. Schematic Representation of the OTFT Sensor Fabrication Process^a

^a On either n^{++} silicon or polyimide substrates with a thin Al film, a 25 nm PVP-HDA dielectric layer was spin-coated, followed thermal evaporation of a 25 nm pentacene active layer and a 35 nm CuPc passivation layer. Source-drain (S-D) electrodes with a width (W) of 1000 μm and length (L) of 50 μm were deposited through a shadow mask. The flow cell was laminated on top of OTFTs for operation in buffer media and biosensing demonstrations.

from poor stability in ambient conditions. In order to achieve a long operation lifetime particularly for biosensing applications, the OTFTs must either incorporate stable organic semiconductors or be passivated against environmental degradation.^{4,26}

This paper reports on a new, robust approach for fabricating high-performance OTFTs with stable operation in water and buffer solutions by incorporating a thin copper phthalocyanine (CuPc) film as a passivation layer as well as a hole injection layer on a pentacene based transistor. Combined with a thin polymer dielectric layer for low-voltage operation, this approach enables the use of a high-mobility but not particularly stable semiconductors for aqueous-stable biological and chemical sensor applications. This greatly broadens the choice of organic semiconductors that can be used for OTFT based aqueous biological and chemical sensing. As a demonstration of concept, solutions of biotin and sodium dodecyl sulfate (SDS) in aqueous buffer media were used to show the potential for sensing with the new bilayer structures.

EXPERIMENTAL SECTION

All materials were received from Sigma Aldrich, unless otherwise stated, and were used as received without further purification. Thin films of poly(4-vinylphenol) (PVP; MW 20 000 g mol^{-1}) cross-linked with 4,4'-(hexafluoroisopropylidene) diphthalic anhydride (HDA) were used as the gate dielectric layer. Pentacene and copper phthalocyanine (CuPc) were used as the active semiconducting layer and the passivation layer, respectively. Biotin (MW 244.32 g mol^{-1} , Alfa Aesar), sodium

dodecyl sulfate (SDS; MW 288.38 g mol^{-1}), and phosphate buffered saline (PBS) tablets were used for the biosensing experiments. The analytes were diluted in freshly prepared phosphate-buffered saline (PBS) solution (10 mM, pH 7.4).

Device Fabrication and Characterization. Highly doped n -type silicon wafers (100) and polyimide (PI) with a thin aluminum sheet (flexible) were used as the common-gate substrates. Both substrate types were cleaned by rinsing with acetone, isopropanol, ethanol, and Milli Q water followed by heating at 100 $^{\circ}\text{C}$ for 5 min. Solutions of PVP were prepared according to a previously reported method⁴ and spin-coated (Headway Research, Inc.) onto substrates at a rate of 7000 rpm for 45 s and baked at 200 $^{\circ}\text{C}$ for 2 h yielding 25 nm cross-linked PVP films. Organic semiconductors pentacene (25 nm) and CuPc (35 nm) were deposited sequentially at room temperature via thermal evaporation (Leybold Vacuum System; UNIVEX 300) at a rate of 0.5 \AA s^{-1} under a base pressure of 5×10^{-6} mbar and then annealed at 170 $^{\circ}\text{C}$ for 1 h. Gold source-drain electrodes were evaporated through a shadow mask with a channel width (W) of 1000 μm and length (L) of 50 μm . The flowchart for the fabrication of OTFTs is shown in Scheme 1.

The surface morphology of the organic films was examined by atomic force microscopy (AFM; NanoScope Dimension 3100 CL) and scanning electron microscopy (SEM; Leo 1530 Gemini). The structural order within the films was characterized by X-ray diffraction (XRD; Bruker AXS D8 diffractometer and X-ray diffractometer 3003 Seifert/GE). All electrical measurements were performed with a Keithley 4200 Semiconductor Characterization System in ambient air and aqueous media.

Electrical sensing measurements were performed under constant bias conditions ($V_{\text{DS}} = -0.5$ V and $V_{\text{G}} = -1$ V). A home-built flow cell

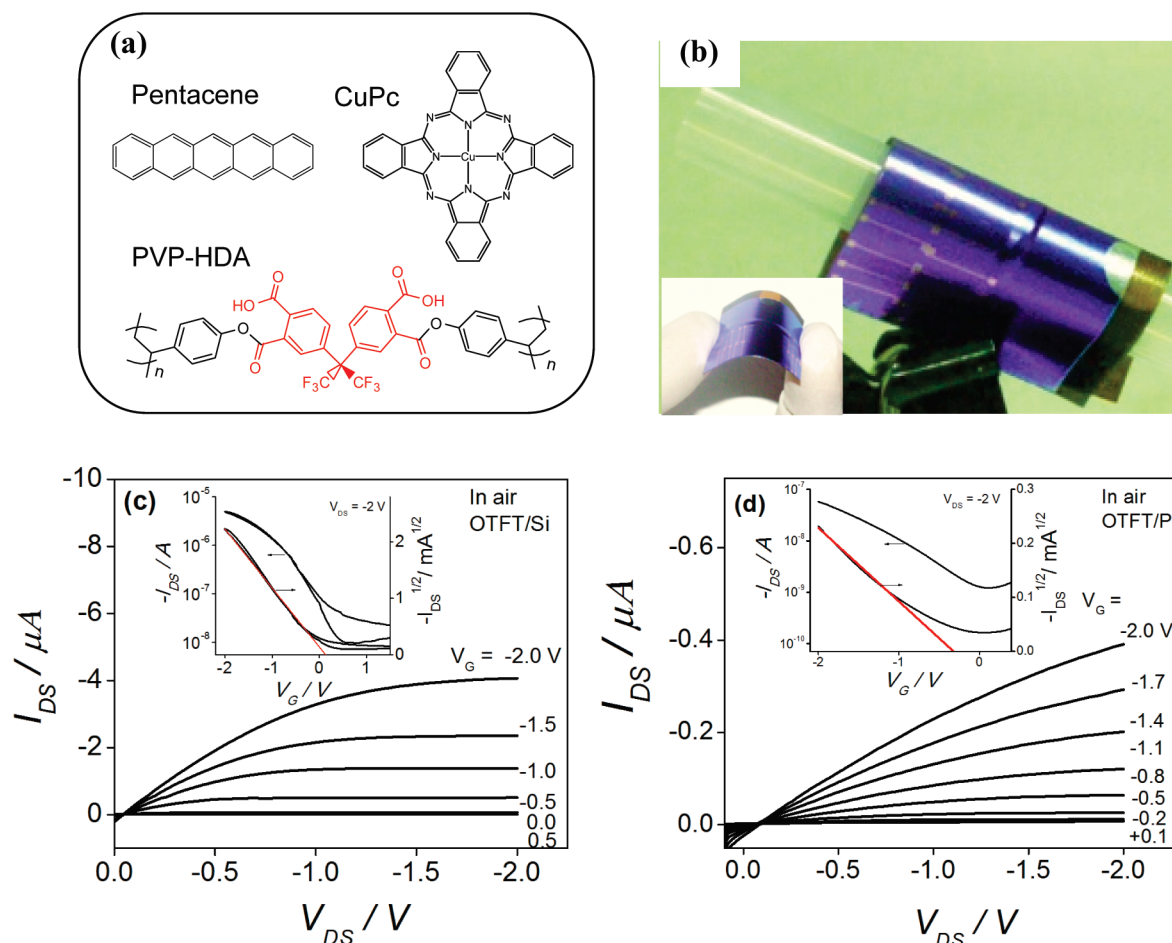


Figure 1. Electrical characteristics of a top-contact OTFT with CuPc (35 nm) and pentacene (25 nm) on a PVP-HDA (25 nm) gate insulator with W/L of 20 using either Si or polyimide (PI) as the substrate. (a) Chemical structures of pentacene, CuPc, and the cross-linked PVP-HDA dielectric. (b) Digital photograph of a flexible OTFT while bent around a syringe. (c) Output characteristics (I_{DS} vs V_{DS}) with various V_G and (inset) transfer characteristics (I_{DS} vs $V_G = -2$ V) using Si as a substrate. (d) Current–voltage output plot as a function of V_G and (inset) transfer characteristics (I_{DS} vs $V_G = -2$ V) on a PI (flexible) substrate.

constructed with Plexiglas was used to confine the buffer and analyte solutions to the surface of the OTFT channel region. The contact areas were sealed with a Viton O-ring, and the flow channel was connected to a peristaltic pump (NovoChem) using Tygon tubing with an inner diameter of 0.76 mm. The peristaltic pump delivered solution from the sample reservoirs at a constant rate of $300 \mu\text{L min}^{-1}$ to ensure a constant analyte concentration. After allowing the current to stabilize under the constant bias conditions (baseline), the flow was switched to the analyte and the current was measured until the saturated response was observed.

RESULTS AND DISCUSSION

OTFT Operation in Ambient Air. Top-contact OTFTs were fabricated with organic semiconductor pentacene on an ultrathin cross-linked poly(4-vinylphenol) (PVP) dielectric layer. Pentacene was chosen as the active layer, because of its relatively high mobility and wide use for circuits and vapor sensors.²⁷ The chemical structures of the semiconducting and polymer insulating layers are shown in Figure 1a. The PVP insulating films cross-linked with 4,4'-(hexafluoroisopropylidene) diphthalic anhydride (HDA) have previously been proven stable toward air and water and showed current densities below 10^{-7} A/cm^2 at gate bias (V_G) = -1 V. The dielectric constant does not vary significantly with cross-linker and is most influenced by the PVP

matrix. The values are slightly higher, i.e., $k = 4.1$, than the dielectric constant reported for PVP.^{5,8,28} They also have a low surface roughness of 0.2 nm, as determined by atomic force microscopy (AFM; Supporting Information Figure SI.1). Previous reports have also shown that it is necessary to use thin dielectric films in OTFTs to achieve low-voltage operation, which is essential for operating in aqueous based systems without encapsulating the source-drain electrodes.⁴ Biosensing applications also require semiconductor materials with stability in ambient air and aqueous media; however, to circumvent this restriction, we incorporated a thin passivation layer comprising a stable organic semiconductor, CuPc, on the surface of the pentacene active layer (see Scheme 1 for device structure fabrication scheme). In our device construction, CuPc serves two functions: passivating the pentacene surface and enhancing charge carrier injection from the electrode. Previously, CuPc films have been used to enhance the hole injection and transport layer in organic light emitting diodes (OLEDs)²⁹ and organic photovoltaics cells.³⁰ Several reports have demonstrated that the hole-injection efficiency can be enhanced by incorporating an interfacial layer between the electrode and the semiconductor in a top contact configuration.^{31,32} In our approach, a thin CuPc layer is evaporated on the pentacene semiconductor layer before

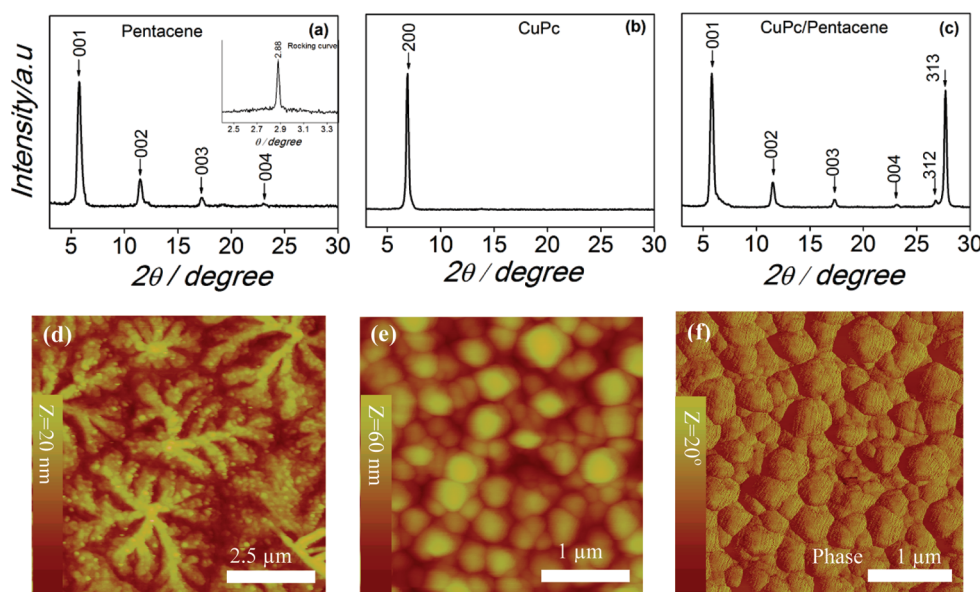


Figure 2. XRD profiles and AFM images on Si substrates. (a) Pentacene (25 nm)/PVP-HDA, (inset) rocking curve from pentacene film at Bragg reflection (001), (b) CuPc (35 nm)/PVP-HDA, and (c) CuPc (35 nm)/pentacene (25 nm)/PVP-HDA. (d) AFM height images showing the morphology of pentacene (25 nm)/PVP-HDA, (e) CuPc (35 nm)/pentacene (25 nm)/PVP-HDA, and (f) phase image of e.

the gold electrodes. An energy level diagram of the Au/pentacene and Au/CuPc/pentacene interface is shown in the Supporting Information, Figure SI.2. The injection barrier between Au and CuPc is slightly smaller than the barrier between Au and pentacene. If we assume that no interface dipole is formed between CuPc and pentacene, the injection barrier is indeed smaller after incorporating a thin layer of CuPc.³¹ It has also been found that densely packed thin-films of face-on oriented CuPc molecules favor charge transport normal to the substrate.³³

The thickness of each layer, pentacene and CuPc, was optimized to obtain the highest effective charge-carrier mobility (μ_{eff}) in the pentacene layer. Figure 1c shows the output characteristics ($I_{\text{DS}}-V_{\text{DS}}$) of a typical p-channel pentacene transistor with a CuPc top layer at various gate voltages (V_{G}). The source-drain current (I_{DS}) was also measured as a function of V_{G} at a constant V_{DS} and used to extract the critical device parameters, including the saturation mobility (μ), current on/off ratio, and threshold voltage (V_{th}). Forward and reverse V_{G} bias sweeping reveals minor hysteresis, as shown in the inset of Figure 1c, which can be attributed to charge trapping or charging near the organic semiconductor/dielectric interface.³⁴ However, few reports showed a long-term stable behavior of pentacene transistors with insulating passivation, but the thickness of those encapsulations is high enough to screen the sensing properties.^{35,36} Devices fabricated on planar Si substrates exhibited an average field-effect mobility of $1.15 \pm 0.2 \text{ cm}^2 \text{ V}^{-1} \text{ s}^{-1}$ at -2 V , while those on polyimide (PI)/Al gate substrates measured on a flat stage (Figure 1d) displayed values of $0.022 \pm 0.2 \text{ cm}^2 \text{ V}^{-1} \text{ s}^{-1}$ under the same bias conditions. Optical images of the flexible OTFTs fabricated on PI/Al are shown in Figure 1b. Mobility values approaching $0.08 \pm 0.01 \text{ cm}^2 \text{ V}^{-1} \text{ s}^{-1}$ could be achieved on PI/Al substrates at an increased gate bias of -5 V (Supporting Information, Figure SI.3). The roughness (rms = 12.5 nm) of the CuPc passivation layer appears similar on both substrates; however, the grains of the underlying pentacene layer were smaller on the flexible PI/Al substrates (Supporting Information, Figure SI.4a,b (PI/Al)). The lower performance can, therefore, be

attributed to the rougher substrate with smaller pentacene grains and less uniform gate-dielectric layer, which is typically observed when transferring devices to rougher plastic substrates.

OTFTs were also fabricated with pentacene active layers without the CuPc passivation layer and annealed at 170°C in ambient air. The electrical performance of these devices was inferior to those with a CuPc injection layer, with a mobility of $0.15 \text{ cm}^2 \text{ V}^{-1} \text{ s}^{-1}$ at an operating voltage of -2 V (Figure SI.5 (Supporting Information) shows the transfer characteristic). This result indicates that the improved performance of bilayer transistor devices is due to the CuPc encapsulation layer that subsequently reduces the energy barrier for charge injection and reduces the contact resistance.

Structural Characterization. X-ray diffraction (XRD), scanning electron microscopy (SEM), and atomic force microscopy (AFM) were used to investigate the structure and morphology of the CuPc modification layer on the pentacene thin-films. Figure 2a–c shows XRD profiles of pentacene (25 nm)/PVP-HDA, CuPc (35 nm)/PVP-HDA, and CuPc (35 nm)/pentacene (25 nm)/PVP-HDA structures measured in the θ - 2θ mode. The peaks of the as-deposited pentacene films were fit to a series of (00 l) lines ($l = 1-4$) with a spacing of 15.3 Å, and no bulk phase was observed (Figure 2a). This indicates that the long axis (c^*) of pentacene molecules is perpendicularly aligned to the surface with a layered structure.³⁷ The crystalline parameters, including the domain size and degree of structural disorder, were determined from the half width of the diffraction peak by analyzing the rocking curve (inset Figure 2a). The calculated value for the full-width at half-maximum (FWHM) was 0.03° , which is consistent with a lower limit domain size of approximately 50 Å, as determined by the Scherrer formula $D = K\lambda/\Delta\cos\theta$, neglecting contributions of line broadening.³⁸

A diffraction peak at $2\theta = \sim 6.9^\circ$ from the CuPc layer on PVP-HDA (Figure 2b) is consistent with reported values,³⁹ generally labeled as the (200) diffraction for the α -phase. Molecular packing of planar phthalocyanines, in particular, CuPc, in the solid state shows a broad polymorphism. The most frequent

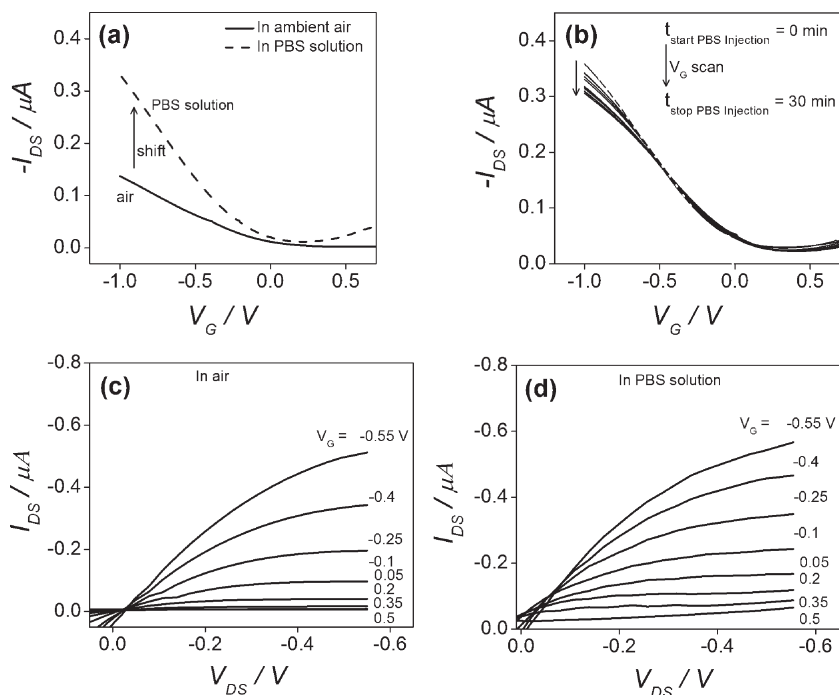


Figure 3. Electrical characteristics of a representative top-contact OTFT with CuPc (35 nm) and pentacene (25 nm) on a PVP-HDA (25 nm) gate dielectric layer with gold source-drain electrodes ($W/L = 20$) on an $n++$ Si gate/substrate. (a) Transfer characteristics (I_{DS} vs V_G) with a constant V_{DS} of -1 V in ambient air (black solid curve), immediately after the injection of a buffer solution with a flow rate of $300 \mu\text{L min}^{-1}$ (blue dashed curve). (b) Transfer characteristics (I_{DS} vs V_G) while in buffer solution for 30 min, showing almost no change in V_{th} and on/off with time. Output characteristics (I_{DS} vs V_{DS}) are shown for an OTFT in (c) ambient air and (d) under aqueous conditions.

forms, α and β , have been studied extensively.⁴⁰ The scattering curve for the bilayer structure comprising CuPc on pentacene is shown in Figure 2c. It can be seen that the 200 diffraction peak associated with CuPc disappeared. Instead, two diffraction peaks appeared at $2\theta \sim 27.58^\circ$ ($d \sim 3.2 \text{ \AA}$) and $\sim 26.75^\circ$ ($d \sim 3.33 \text{ \AA}$). The first peak can be fit to the (313) lattice plane, and the other can be fit to the (312) lattice plane. Hence, this $3.2 \text{ \AA}/(313)$ diffraction peak is most accurately assigned to α -CuPc crystallites, consistent with a standing b -axis. Since, the peak at $3.33 \text{ \AA}/(312)$ is always observed with the $3.2 \text{ \AA}/(313)$ peak in the α -polymorph, it seems very plausible to associate it with α -CuPc or a very close relative to α -CuPc.^{41,42} In the bilayer configuration (Figure 2c), the diffraction peaks from pentacene did not shift and showed an identical symmetry to the diffraction peaks as displayed in Figure 2a. Thus, the high mobility of pentacene can be attributed to the thin-film phase of pentacene with highly oriented molecules normal to the substrate, as evidenced from the sole (100) peak at $2\theta = 5.7^\circ$ and the absence of a bulk phase.

Atomic force microscopy (AFM) images are shown in Figure 2d,e, for pentacene/PVP-HDA and CuPc/pentacene/PVP-HDA, with surface roughness (rms) values of 5 and 12 nm, respectively. The AFM images of a CuPc film deposited on pentacene shows face-on orientation either in columnar structures or within rodlike crystals (Figure 2e). Figure 2f shows the densely packed structure of such a face-on crystal that was further confirmed by the SEM (edge view, Figure SI. 6, Supporting Information). The stable electrical measurements of these devices in air (Figure 1c) are likely directly related to the densely packed array of domains with a homogeneous CuPc film as the top layer. The highly compact and oriented nature of the CuPc grains suggest that buffer solution penetration into the film will be minimized when applying these transistors as a biosensing platform.

OTFT Operation in Buffer Solution. OTFT stability in aqueous media was characterized using the flow system described in the Experimental Section. A flow cell was laminated on the surface of an OTFT such that the solution chamber primarily contacted the channel region. Freshly prepared 10 mM phosphate buffered saline (PBS) solution with pH 7.4 was injected into the channel, and electrical measurements were performed in a similar manner to ambient measurements. Compared to ambient air, we observed an increase in both on- and off-currents and a shift in the threshold voltage (V_{th}) from 0.4 to 0.3 V (Figure 3a) when operating the device in buffer solution. The operational stability in buffer solution was investigated by measuring the transfer characteristics ($V_{DS} = -1$ V) over a period of 30 at 2.5 min intervals; the results are featured in Figure 3b. Only a small change in I_{DS} was observed over the given time period, which can be attributed to the increasing relative humidity at the interface, in agreement with previous results.^{5,43,44} Remarkably, the pentacene based transistor with a CuPc layer functioned well in buffer solution, exhibiting only a moderate reduction in mobility from $0.8 \pm 0.2 \text{ cm}^2 \text{ V}^{-1} \text{ s}^{-1}$ (ambient) to $0.5 \pm 0.08 \text{ cm}^2 \text{ V}^{-1} \text{ s}^{-1}$ (aqueous buffer). This indicates the CuPc top layer is effective in protecting the pentacene. Figure 3c,d shows the output characteristics in ambient air and buffer solution, respectively. We expect to see a small shift in I_{DS} (<one time at -0.55 V) when the surface was exposed to buffer solution (Figure 3d), but due to minor leakage, it was invisible. Control OTFTs were fabricated with 50 nm CuPc active layers, and their transfer and output characteristics are presented in the Supporting Information, Figure SI.7a,b, respectively. These devices showed not only low mobility, i.e., $4 \times 10^{-3} \text{ cm}^2 \text{ V}^{-1} \text{ s}^{-1}$, but also low current on/off ratios of 8×10^1 at an applied voltage of -2 V. We previously showed that low

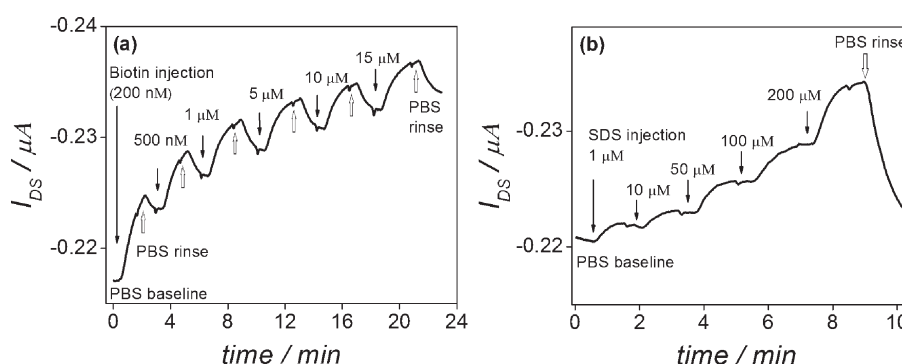


Figure 4. Kinetic/surface titration measurements of biotin and SDS detection using pentacene based OTFT sensors with CuPc top coating. The measurements were performed at constant biasing $V_G = -1$ V and $V_{DS} = -0.5$ V with a flow rate of $300 \mu\text{L min}^{-1}$. Solid arrows indicate the addition of analyte solutions, and open arrows indicate the exchange of the analyte with buffer solutions. OTFT sensor titration using (a) biotin and (b) SDS.

electrical performance devices did not provide adequate sensitivity for use as OTFT sensors⁵ with negligible sensor responses in aqueous media, as shown in Figure SI.7c, Supporting Information. Other recently reported high mobility organic semiconductors may be suitable candidates without encapsulation. However, pentacene is readily available, and the approach here can potentially offer a general approach for high mobility organic transistors to be implemented in water-stable sensors.

Sensor Applications. Label-free detection of biomolecules is possible using organic transistors, which provide an output signal in the form of a change in electrical current in response to a binding event.⁴ The occurrence of chemical or physical absorption is converted to a ΔI_{DS} response, which depends on the analyte composition, concentration, and the OTFT bias conditions.^{4,5} The main challenge is detecting a particular analyte or discriminating between multiple species that may elicit a similar response from a particular organic semiconductor in buffer solution. This requires that specific binding molecules/sites are attached to the surface of the OTFT. Thus, more complex device structures can be prepared in a similar manner to our previously reported paper,⁴ where the surface functionality was achieved using the plasma polymerization of maleic anhydride, because it is applicable to any surfaces.⁴⁵ Nonetheless, it is outside the main scope of this paper. Here, we investigate the transistor response to several biologically relevant chemicals, namely, biotin, pH, and sodium dodecyl sulfate (SDS), as a demonstration of concept for the use of CuPc encapsulated pentacene OTFTs as the readout transistors for future biosensor development.

Various molecules containing primary amines, such as proteins and antibodies, can be covalently attached to create a ligand-functionalized substrate. These chemical reactions can be performed in standard buffer solutions under mild protein structure-protective conditions, which mainly include a pH and ionic strength of buffer solution.^{46,47} Additionally, the strength with which antibody–antigen binds also depends mainly on the pH of the working solution due to the different isoelectric points (pI) of different proteins.⁴⁷ Thus, the influence of pH on these devices was investigated and can be found in the Supporting Information, Figure SI.8. pH sensing in particular shows a typical response time of 50 s and a recovery time 70 s, indicating a good reversible and reproducible characteristic.

Next, we show the detection of biotin due to its wide application in gene therapy,⁴⁸ single-molecule enzymology and nanotechnology, microarrays, microchip based capillary electrophoresis,⁴⁹ and multiplexed protein measurements.⁵⁰ Prior to measuring sensor

responses, a baseline current was recorded for approximately 60 s in the buffer solution. While recording the background current, only a small shift in baseline current was observed (which stabilized within seconds), further demonstrating that CuPc is effective in passivating the pentacene layer toward aqueous media. Biotin solutions with concentrations ranging from 200 nM to $15 \mu\text{M}$ (diluted in buffer solution of pH 7.4) were injected into the flow cell after the current was stabilized in buffer solution while continuously monitoring the OTFT current. After injecting a 200 nM biotin solution, the I_{DS} increased with time until equilibrium was reached between the bulk concentration (C_o) and the corresponding surface coverage. The remaining solutions were sequentially injected (thin arrows), and the OTFT response as a function of analyte concentration is shown in Figure 4a. The adsorption of biotin onto the OTFT surface resulted in an increase in I_{DS} proportional to the increase in equilibrium surface charge density. Upon rinsing, the I_{DS} signal partially decayed toward the initial baseline due to biotin desorption from the surface. It is important to mention here that our OTFT platform does not have surface functionality needed for selective analyte detection. However, the electronic structure of proteins consisting of amino-acids with charged groups are determined by the isoelectric point (pI) of a respective analyte. Since biotin is a highly polar molecule with a pI of 3.5, above the pI, it possess negative charges, and below, it shows average positive charges due to high ratio of NH_2 to NH_3^+ .^{51,52} Therefore, in pH 7.4 (our working solution), biotin can attain negative charges and the CuPc surface has a positive net charge upon exposure to air/liquid.⁵³ We can presume that electrostatic interactions will draw the biotin from solution to the CuPc surface, which results in an increase in OTFT current during sensor measurements. Furthermore, these devices showed a very slow decay in current upon rinsing with buffer solution (Figure 4a), indicating a strong interaction between the surface and adsorbed species. This is consistent with previous literature in which DNA probes were electrostatically adsorbed onto the polylysine matrix/Si-nanowires and the OTFT current response was attributed to a top-gating effect.^{54,55} A similar mechanism may be applied to our sensors via the formation of a negative ion accumulation layer from biotin species adsorbing at the pentacene/CuPc interface. Ion diffusion through the grain boundaries may also result in a change in I_{DS} in OTFT sensors; however, the negatively charge biotin species interacting with the pentacene layer would result in a decrease in I_{DS} ,^{5,51} which is not the case in our sensor measurements. It is, therefore, likely that the analytes are capacitively

interacting with the charge transport layer while being separated by a nonion conducting film, i.e., the CuPc passivation layer. The biotin surface exhibits a surface potential and a related surface charge. This surface potential is known as the Donnan potential,⁵⁶ or the potential between two solutions separated by the membrane. If we consider that the biotin is closely adsorbed to the sensor surface, then the protein species provides only the external potential detected by the transistor sensors. Multiple detection experiments using a 200 nM biotin concentration were measured, and the change in current with time is shown in Supporting Information, Figure SI.9. We conclude from a similar ΔI_{DS} that the sensor surface is stable and can be reused for multiple experiments.

In addition to detecting biotin, we also found that our OTFTs showed sensitivity to chemical additives without degradation. Sodium dodecyl sulfate (SDS) is a negatively charged molecule at pH 7.4 and is commonly used as detergent to remove nonspecific bound protein⁵⁷ and more recently to identify the limit of detection (LOD) in DNA sensors.⁵⁸ It is important to understand its influence on the transistor sensor performance; therefore, we evaluated the sensor response with concentrations applicable to these applications. A clear I_{DS} response was observed for SDS diluted in buffer solutions down to 1 μ M concentration (Figure 4b). The injection of 10, 50, 100, and 200 μ M SDS solutions (thin arrows) resulted in a correspondingly higher I_{DS} as the equilibrium surface coverage increased. Upon rinsing (thick open arrows), the device showed a rapid current decay toward the buffer solution baseline current, which occurred over a period of ~ 60 s. It is worth mentioning that the SDS analyte does not show a chemical or strong physical interaction with the CuPc surface, as the OTFT current rapidly approached the baseline current from buffer solution rinsing alone (Figure 4b). Additional evidence is displayed by the sensor response curves of biotin and SDS; i.e., SDS shows a linear response as the concentration increases compare to biotin response (response proportional to surface coverage (concentration)). Moreover, the transistor showed no degradation, as determined by the consistent current, even at high concentration of SDS.

The above studies demonstrate that our pentacene based transistor with a CuPc encapsulation layer is capable of stable and rapid biochemical detection. Chemical and biological species can be detected, even when a passivation layer is incorporated on the surface of the active semiconductor layer. Other recently reported high mobility organic semiconductors may be suitable candidates without encapsulation.^{4,5} However, pentacene is readily available, and the approach here can potentially offer a general approach for high mobility organic transistors to be implemented in water-stable sensors. Nevertheless, one can easily process these bilayer devices through a dry/solution deposition technique to create the surface functionalities for selective interaction of biospecies.⁴

CONCLUSION

We have demonstrated an approach for integrating CuPc/pentacene bilayer structures as a general method to obtain aqueous-stable transistor sensors. As a result, stable device behavior was achieved in aqueous buffer media with a mobility of up to $0.5 \pm 0.08 \text{ cm}^2 \text{ V}^{-1} \text{ s}^{-1}$, representing one of the highest values reported for OTFTs in aqueous media. These devices benefit from the addition of an organic semiconductor passivation layer with densely packed grains that simultaneously improve device performance via enhanced hole injection and stability toward

aqueous media. Most importantly, our approach allows for the incorporation of water-unstable organic semiconductors as the active transport layer rather than restricting the selection to highly stable materials. The biosensing results presented above show that pentacene based transistor sensors are capable of real-time detection of charged molecules with reversible and reproducible results that are promising for a variety of sensor applications. Future work will examine the selective detection of antibodies, quantify the immunodetection efficiency, and investigate the influence of pH on analyte sensitivity.

ASSOCIATED CONTENT

S Supporting Information. PVP-HDA thin-film characterized by AFM, energy band diagram of pentacene active layer, bare pentacene based transistor characteristics, characterization of pentacene active layer by AFM, and SEM. CuPc based transistor characteristic and pH sensing (PDF). This material is available free of charge via the Internet at <http://pubs.acs.org>.

AUTHOR INFORMATION

Corresponding Author

*Z.B.: e-mail, zbao@stanford.edu; tel, 650-723-2419; fax, 650-723-9780. H.U.K.: e-mail, khanh@mpip-mainz.mpg.de; tel, +49 6131-379549; fax, +49 6131-379100.

ACKNOWLEDGMENT

H.U.K. acknowledges the financial support from International Research Training Group (IRTG 1404/funded by DFG) and Max Planck Society (Germany). M.E.R. acknowledges partial support from the NASA GSRP fellowship. Z.B. acknowledges partial support from the National Science Foundation (NSF ECCS-0730710) and Office of Naval Research (N000140810654). We thank to Dr. V. Enkelmann, Max Planck Institute for Polymer Research, Mainz, Germany, for fruitful discussion on XRD data. We also thanks to Dr. K. P.-Kamloth and Dr. J. Wüsten, IMM, Mainz, Germany, for provision of organic materials evaporator.

REFERENCES

- (1) Friend, R. H.; Gymer, R. W.; Holmes, A. B.; Burroughes, J. H.; Marks, R. N.; Taliani, C.; Bradley, D. D. C.; Santos, D. A. D.; Brédas, J. L.; Lögdlund, M.; Salaneck, W. R. *Nature* **1999**, 397, 121.
- (2) Wohrle, D.; Meissner, D. *Adv. Mater.* **1991**, 3, 129.
- (3) Steudel, S.; Myny, K.; Arkhipov, V.; Deibel, C.; Vusser, S. D.; Genoe, J.; Heremans, P. *Nat. Mater.* **2005**, 4, 597.
- (4) Khan, H. U.; Roberts, M. E.; Johnson, O.; Förch, R.; Knoll, W.; Bao, Z. *Adv. Mater.* **2010**, 22, 4452.
- (5) Roberts, M. E.; Mannsfeld, S. C. B.; Queralto, N.; Reese, C.; Locklin, J.; Knoll, W.; Bao, Z. *Proc. Natl. Acad. Sci. U.S.A.* **2008**, 105, 12134.
- (6) Sokolov, A. N.; Roberts, M. E.; Bao, Z. *Mater. Today* **2009**, 12, 12.
- (7) Bao, Z.; Dodabalapur, A.; Lovinger, A. J. *Appl. Phys. Lett.* **1996**, 69, 4108.
- (8) Roberts, M. E.; Queralto, N.; Mannsfeld, S. C. B.; Reinecke, B. N.; Knoll, W.; Bao, Z. *Chem. Mater.* **2009**, 21, 2292.
- (9) Ling, M. M.; Bao, Z. *Chem. Mater.* **2004**, 16, 4824.
- (10) Bettinger, C. J.; Bao, Z. *Adv. Mater.* **2010**, 22, 651.
- (11) Zschieschang, U.; Yamamoto, T.; Takimiya, K.; Kuwabara, H.; Ikeda, M.; Sekitani, T.; Someya, T.; Klauk, H. *Adv. Mater.* **2011**, 23, 654.
- (12) Hwang, H. S.; Zakhidov, A. A.; Lee, J.-K.; André, X.; DeFranco, J. A.; Fong, H. H.; Holmes, A. B.; Malliaras, G. G.; Ober, C. K. *J. Mater. Chem.* **2008**, 18, 3087.

- (13) Ortiz, R. P.; Facchetti, A.; Marks, T. J. *Chem. Rev.* **2010**, *110*, 205.
- (14) Tsao, H. N.; Muellen, K. *Chem. Soc. Rev.* **2010**, *39*, 2372.
- (15) Berggren, M.; Richter-Dahlfors, A. *Adv. Mater.* **2007**, *19*, 3201.
- (16) Tanese, M. C.; Fine, D.; Dodabalapur, A.; Torsi, L. *Biosens. Bioelectron.* **2005**, *21*, 782.
- (17) Huang, J.; Miragliotta, J.; Becknell, A.; Katz, H. E. *J. Am. Chem. Soc.* **2007**, *129*, 9366.
- (18) Stern, E.; Klemic, J. F.; Routenberg, D. A.; Wyrembak, P. N.; T.-Evans, D. B.; Hamilton, A. D.; LaVan, D. A.; Fahmy, T. M.; Reed, M. A. *Nature* **2007**, *445*, 519.
- (19) Zhang, G.-J.; Chua, J. H.; Chee, R.-E.; Agarwal, A.; Wong, S. M.; Buddharaju, K. D.; Balasubramanian, N. *Biosens. Bioelectron.* **2008**, *23*, 1701.
- (20) Sun, J.; Zhang, B.; Katz, H. E. *Adv. Funct. Mater.* **2011**, *21*, 29.
- (21) Ha, Y.-G.; Jeong, S.; Wu, J.; Kim, M.-G.; Dravid, V. P.; Facchetti, A.; Marks, T. J. *J. Am. Chem. Soc.* **2010**, *132*, 17426.
- (22) Harting, H.; Zhang, J.; Gamota, D. R.; Britton, D. T. *Appl. Phys. Lett.* **2009**, *94*, 193509.
- (23) Zhu, Z.-T.; Mason, J. T.; Dieckmann, R.; Malliaras, G. G. *Appl. Phys. Lett.* **2002**, *81*, 4643.
- (24) Bao, Z.; Locklin, J. J. *Organic Field-Effect Transistors*; CRC Press: Boca Raton, FL, 2007.
- (25) Lin, Y. Y.; Gundlach, D. J.; Nelson, S. F.; Jackson, T. N. *IEEE Electron Device Lett.* **1997**, *18*, 606.
- (26) Jung, H.; Lim, T.; Choi, Y.; Yi, M.; Won, J.; Pyo, S. *Appl. Phys. Lett.* **2008**, *92*, 163504.
- (27) Ling, M.; Bao, Z.; Li, D. *Appl. Phys. Lett.* **2006**, *88*, 033502.
- (28) Halik, M.; Klauk, H.; Zschieschang, U.; Schmid, G.; Radlik, W.; Weber, W. *Adv. Mater.* **2002**, *14*, 1717.
- (29) Mitschke, U.; Bauerle, P. J. *Mater. Chem.* **2000**, *10*, 1471.
- (30) Yang, F.; Shtein, M.; Forrest, S. R. *Nat. Mater.* **2005**, *4*, 37.
- (31) Chen, F.-C.; Kung, L.-J.; Chen, T.-H.; Lin, Y.-S. *Appl. Phys. Lett.* **2007**, *90*, 073504.
- (32) Hu, W. S.; Weng, S. Z.; Tao, Y. T.; Liu, H. J.; Lee, H. Y. *Org. Electron.* **2008**, *9*, 385.
- (33) Resel, R.; Ottmar, M.; Hanack, M.; Keckes, J.; Leising, G. *J. Mater. Res.* **2000**, *15*, 934.
- (34) Park, D.-W.; Lee, C. A.; Jung, K.-D.; Kim, B.-J.; Park, B.-G.; Shin, H.; Lee, J. D. *Jpn. J. Appl. Phys.* **2007**, *46*, 2640.
- (35) Kim, W. J.; Koo, W. H.; Jo, S. J.; Kim, C. S.; Baik, H. K.; Lee, J.; Im, S. *Jpn. J. Appl. Phys.* **2005**, *44*, L1174.
- (36) Pannemann, C.; Diekmann, T.; Hilleringmann, U.; Schurmann, U.; Scharnberg, M.; Zaporozhchenko, V.; Adelung, R.; Faupel, F. *Mater. Sci.-Poland* **2007**, *25*, 95.
- (37) Chou, W.-Y.; Kuo, C.-W.; Cheng, H.-L.; Chen, Y.-R.; Tang, F.-C.; Yang, F.-Y.; Shu, D.-Y.; Liao, C.-C. *Appl. Phys. Lett.* **2006**, *89*, 112126.
- (38) Lukas, S.; Söhnchen, S.; Witte, G.; Woll, C. *ChemPhysChem* **2004**, *5*, 266.
- (39) Liu, G.; Gredig, T.; Schuller, I. K. *Europhys. Lett.* **2008**, *83*, 56001.
- (40) Guillaud, G.; Simon, J.; Germain, J. P. *Coord. Chem. Rev.* **1998**, *180*, 1433.
- (41) Debe, M. K.; Kam, K. K. *Thin Solid Films* **1990**, *186*, 289.
- (42) Naito, R.; Toyoshima, S.; Ohashi, T.; Sakurai, T.; Akimoto, K. *Jpn. J. Appl. Phys.* **2008**, *47*, 1416.
- (43) Chen, F.; Xia, J.; Tao, N. *Nano Lett.* **2009**, *9*, 1621.
- (44) Göllner, M.; Huth, M.; Nickel, B. *Adv. Mater.* **2010**, *22*, 4350.
- (45) Sreenivasan, R.; Gleason, K. K. *Chem. Vap. Deposition* **2009**, *15*, 77.
- (46) Lahiri, J.; Isaacs, L.; Tien, J.; Whitesides, G. M. *Anal. Chem.* **1999**, *71*, 777.
- (47) Carvalho, L. A.; Carmona-Ribeiro, A. M. *Langmuir* **1998**, *14*, 6077.
- (48) Agrawal, S.; Iyer, R. P. *Curr. Opin. Biotechnol.* **1995**, *6*, 431.
- (49) Chiem, N. H.; Harrison, D. J. *Electrophoresis* **1998**, *19*, 3040.
- (50) Kingsmore, S. F. *Nat. Rev. Drug Discovery* **2006**, *5*, 310.
- (51) Kim, D.-S.; Park, J.-E.; Shin, J.-K.; Kim, P. K.; Lim, G.; Shoji, S. *Sens. Actuators, B* **2006**, *117*, 488.
- (52) Vandamme, E. J. *Biotechnology of vitamins, pigments, and growth factors*; Elsevier Science Publishing, London, 1989.
- (53) Yang, M.; Wang, D.; Peng, L.; Xie, T.; Zhao, Y. *Nanotechnology* **2006**, *17*, 4567.
- (54) Bunimovich, Y. L.; Shin, Y. S.; Yeo, W.-S.; Amori, M.; Kwong, G.; Heath, J. R. *J. Am. Chem. Soc.* **2006**, *128*, 16323.
- (55) Fritz, J.; Cooper, E. B.; Gaudet, S.; Sorger, P. K.; Manalis, S. R. *Proc. Natl. Acad. Sci. U.S.A.* **2002**, *99*, 14142.
- (56) Bergveld, P. *Sens. Actuators* **1996**, *A56*, 65.
- (57) Liu, S.; Vareiro, M. M. L. M.; Fraser, S.; Jenkins, A. T. A. *Langmuir* **2005**, *21*, 8572.
- (58) Chu, L.-Q.; Knoll, W.; Foerch, R. *Biosens. Bioelectron.* **2008**, *24*, 118.